IRSTI 47.05.17 https://doi.org/10.26577/ijmph.2023.v14.i2.08

A.M. Abdelaziz [1], I.E. Molotov [2], S.K. Tealib[1,*]

[1] National Research Institute of Astronomy and Geophysics (NR IAG), Helwan, Egypt
[2] Keldysh Institute of Applied Mathematics, Moscow, Russia.
*e-mail: shafeeq.taelib@nriag.sci.eg
(Received 24 November 2023; accepted 20 December 2023)

Accurate High-Altitude Orbit Determination Method using Electro-Optical Sensors

Abstract. This paper presents an approach to accurately determine the orbits of Medium Earth Orbit (MEO) and Geosynchronous Earth Orbit (GEO) space objects by utilizing data from an electro-optical sensor (Optical Satellite Tracking Station (OSTS), Kottamia Observatory station). The proposed method combines an extended and unscented Kalman filter with a semi-analytical propagation model. The effectiveness of this approach is demonstrated through numerical simulations and comparisons with traditional orbit determination techniques. The results drawn from this study show that when comparing both methods, the unscented semi-analytical Kalman filter provided more accurate orbital state estimates and required less time and fewer observations to converge.
Keywords: orbit determination; orbit propagation; extended semi-analytical Kalman filter; unscented semi-analytical Kalman Filter; optical observations.

Introduction

The accurate determination of the orbits of space objects is of utmost importance for both space situational awareness and collision avoidance. While electro-optical sensors offer valuable tracking data, the presence of high noise and measurement uncertainties poses significant challenges to achieving precise orbit determination. To determine the orbits of space objects as accurately as possible, optical telescopes are employed to provide tracking data. However, it is important to note that this type of observation has limitations in coverage due to environmental and mechanical constraints. Consequently, the number of observations available for space objects is restricted based on factors such as their position, velocity, orientation, and size. The process of orbit determination holds a crucial role in a catalog maintenance system [1]. By addressing the difficulties associated with accurate orbit determination, this research seeks to enhance space object tracking and collision avoidance measures. The Orbit Determination (OD) problem involves determining the state of a satellite as a function of time using measurements obtained from ground-based tracking stations [2-3]. This process requires the accurate prediction of an orbit based on initial conditions and the application of estimation algorithms [4], especially when dealing with nonlinear problems. To improve computational efficiency and accuracy, the Semi-analytic Satellite Theory, which employs the Batch Least Squares and the extended Kalman filter methods was introduced by [5]. This approach enhances the speed of orbit determination systems by optimizing the propagator's computational efficiency. Additionally, [6] explored the extended semi-analytic Kalman filter, which combines the traditional extended Kalman filter with Draper Semi-analytic Satellite Theory (DSST). This models both short-periodic motions and the mean elements of the satellite orbit. Furthermore, [7] utilized coupled Draper Semi-analytic Satellite Theory with a Backward Smoothing Extended Kalman Filter. In [8] a study on the analytical implementation of the extended Kalman filter for orbit determination. They derived analytical solutions for the state transition matrix. [9] Used a second-order extended Kalman filter after the observations of multi-spacecraft tracking for accurate measurement prediction. This paper addresses the problem of sequentially performing real-time orbit determination for medium earth orbit and geostationary earth orbit satellites. This paper aims to tackle these challenges through the introduction of an

innovative orbit determination technique. The primary objective is to compare the attitude estimation outcomes between the extended semi-Kalman filter (ESKF) and the unscented semi-Kalman filter (USKF) of an artificial satellite using real data from ground stations. The paper will also conduct a comprehensive review of existing methods for orbit determination, utilizing data from various sensors, while highlighting their respective limitations and advantages. Moreover, conventional Kalman filter-based approaches will be discussed, with a specific emphasis on the necessity for improvements to effectively handle complex space object dynamics. The proposed methodology will include the process of initial orbit determination and Semi-analytical estimation. Finally, the paper will present and analyze the results concerning the position and velocity of the root mean square (RMS).

The Initial Orbit Determination

Initial Orbit Determination (IOD) is the process of estimating the initial orbital parameters of a satellite or spacecraft shortly after its launch or deployment into space. IOD methods depend on a limited set of observations and are used to calculate the first estimate of an object's orbit. So, these methods usually operate simplified orbital dynamics and thus neglect perturbations. The Apex-II software package is used [10] for the image processing observed, the state vectors of the objects were determined for each series by the Double-r iteration method, for more details refer to the reference [11].

1.1 Nonlinear Filtering

The available measurement points during one calculation are used to determine a result at a specified reference time by employing Kalman Filters adapted for a nonlinear system to compute the orbits. In this context, the Kalman Filter updates the reference trajectory only after processing all observations. On the other hand, the extended Kalman filter updates the reference trajectory after processing each measurement, as mentioned by [12]. Now, let the system be modeled in the following nonlinear form according to [13].

$$\dot{x}(t) = f(x(t),t) + \omega(t), \quad t > 0 \tag{1}$$

$$y(t_k) = h_d(x(t_k),t_k) + \nu(t_k), \quad k = 0,1,2,3,.... \tag{2}$$

where $x(t) \in \mathbb{R}^n \ \ and \ \ \omega(t) \in \mathbb{R}^n$are, respectively, the state vector and the continuous process noise at time t, $y(t_k) \in \mathbb{R}^m \ \ and \ \ \nu(t_k) \in \mathbb{R}^m$are, respectively, the measured output and the discrete measurement noise at discrete times $t_{k.}$ $f: \mathbb{R}^n \times \mathbb{R}^+ \ \mapsto \mathbb{R}^n$ is the system's dynamic function and $h_d: \mathbb{R}^n \times \mathbb{R}^+ \ \mapsto \mathbb{R}^n$ is the measurement function. Process noise represents both the disturbances that are unmolded because they are unknown, as well as those intentionally excluded due to model complexity or computational limitations.

The discretization is being performed considering noiseless state dynamics by setting. $\omega(t) = 0$, then adding the discretized process noise $\omega_d(t_k)$ to equation (1):

$$x(t_{k+1}) = f_d(x(t_k),t_k) + \omega_d(t_k), \quad k = 0,1,... \tag{3}$$

The concept of stochastic discretization of nonlinear dynamics in the context of Kalman estimation is further explored in representing the Semi-analytical orbital propagation model of the mean dynamics. That accounts for the uncertainty error in the mean state propagation and therefore may be written in the same functional form as Equation (3).

$$\dot{\bar{\zeta}}(t)(t) = \bar{f}(\bar{\zeta}(t),t) + \bar{\omega}(t) \tag{4}$$

where $\bar{\zeta}(t)$ are the mean elements at a certain epoch t, $\bar{f}$ is Mean orbital state function and $\bar{\omega}(t)$ is the process noise.

1.2 Extended and Unscented Semi-Analytical Kalman Filter

The extended and unscented semi-analytical Kalman filter represents a fusion of diverse techniques aimed at achieving precise orbit determination. In this context, a semi-analytical orbit determination system is put forth. This system incorporates an orbit propagator that draws from the principles of Semi-analytical Satellite Theory and employs an extended sequential estimator. The orbit propagation theory derived from Semi-analytical Satellite Theory encompasses two key components: the Averaged Orbit Generator and the Short Periodic Generator. These components facilitate efficient and accurate large-step size propagation by effectively separating the satellite's long-period and secular motion [14]. To complement the distinctive averaged

formulation of the satellite's equations of motion as defined in Semi-analytical Satellite Theory, an Extended Semi-analytical Kalman Filter has been developed by [6] and [15]. The a posteriori state is expressed as follows:

$$\overline{\xi}^{+}\left(t_{k,\mathrm{m}}\right)=\overline{\xi}_{N}\left(t_{k,\mathrm{m}}\right)+\Delta\overline{\xi}^{k,\mathrm{m}}_{k,m}$$
$$k=\ 0,\ 1, and\ m=1,...,\ 6\ indexes\ of\ ECI\ frame) \quad (5)$$

where $\overline{\xi}^{+}\left(t_{k,\mathrm{m}}\right)$ is the nominal state and $\Delta\overline{\xi}^{k,\mathrm{m}}_{k,\mathrm{m}}$ is the filter correction after the measurement at time $t_{k,m}$.

The anticipated state at the subsequent observation time $t_{k,i+1}$ is provided as follows:

$$\overline{\xi}^{+}\left(t_{k,\mathrm{m}+1}\right)=\overline{\xi}_{N}\left(t_{k,\mathrm{m}+1}\right)+\Delta\overline{\xi}^{k,\mathrm{m}+1}_{k,\mathrm{m}+1} \quad (6)$$

The Unscented Kalman Filter is an extension of the traditional Kalman filter that can handle nonlinear systems more effectively by propagating sigma points (representative points) through the nonlinear functions. This approach enables more accurate and robust estimation in scenarios where traditional linear methods may fall short [16]. The discretization of Equation (4) is performed by integrating between the nominal times $t_{k,0}$ and $t_{k+1,0}$, using Equation (3).

$$\overline{\zeta}_{N}\left(t_{k+1.0}\right)=\overline{f}_{d}\left(\overline{\zeta}_{N}\left(t_{k+1,0}\right),t_{k,0}\right)+\overline{\omega}_{k,0} \quad (7)$$

where $\bar{\omega}_{k,0}$ is the discretized process noise.

Propose incorporating the Semi-analytical propagator and the Unscented Kalman Filter together after each observation is processed. This will allow for the correction of the filter to be propagated using linearized dynamics based on the nominal trajectory.

The root mean square of the position differences between measured and estimated orbits for *n* observation vectors can be expressed as follows:

$$RMS=\sqrt{\frac{1}{n}\sum_{m=0}^{n}\left(\left|\boldsymbol{x}_{meas}-\boldsymbol{x}_{pred}\right|_{m}\right)^{2}} \quad (8)$$

The result of the equation above indicates that a lower Root Mean Square value corresponds to measurement points that are closer to the estimated orbit. Therefore, a low RMS value serves as an indication that the chosen dynamics are valid for the Orbit Determination process. By synergizing the capabilities of Extended Kalman Filtering and Unscented Kalman Filtering [17], we can achieve superior accuracy and resilience in orbit determination. This becomes particularly advantageous when addressing the complexities introduced by nonlinearities in the system, enhancing the overall reliability of the orbit determination process. [18].

Numerical results and discussions

This section is dedicated to presenting pivotal data crucial for precise satellite orbit prediction. The electro-optical sensor plays a central role by capturing high-resolution images of the celestial object in motion. Through the utilization of the Kottamia Observatory, these images provide valuable information regarding the apparent position and dynamic motion of the satellite.

It's noteworthy that the geodetic location of the simulation environment, crucial for the accuracy of the study, is anchored at the Kottamia Observatory in Egypt. The Optical Satellite Tracking Station at this observatory [19] is instrumental in establishing the geodetic framework necessary for the simulation. This reliance on the Optical Satellite Tracking Station enhances the reliability and precision of the study's findings, contributing to the overall effectiveness of the satellite orbit prediction methodology.

The observatory is strategically positioned at a ground location with precise geographical coordinates: latitude 29.933° N, longitude 31.8823° E, and an altitude of 470 meters. Table 1 consolidates the essential parameters for the observed satellites, encompassing the semi-major axis, inclination, eccentricity, and reference time (UT). These parameters correspond to MEO space objects identified by the Two Line Element (TLE) catalog, with IDs 32393 and 40889, as well as GEO space objects from the TLE catalog, with IDs 29648 and 32294 [source: https://www.space-track.org/#gp]. This detailed tabulation serves as a comprehensive reference for the specific satellite characteristics utilized in our observations, facilitating accurate and informed analysis.

Table 1 – Satellites parameters

Date / Time	Object/ ID	Eccentricity (e)	Semi-major axis (a) km	Inclination (*i*) degree
08/07/2021 18:00:00	COSMOS (32393)	0.000139	25511.556	64.4571
11/07/2021 20:00:00	GALILEO 9 (40889)	0.000279	29599.791	55.8573
30/08/2021 20:00:00	MEASAT 3 (29648)	0.000125	42268.9677	0.2218
28/11/2021 19:00:00	SKYNET 5B (32294)	0.000363	42166.5295	1.0226

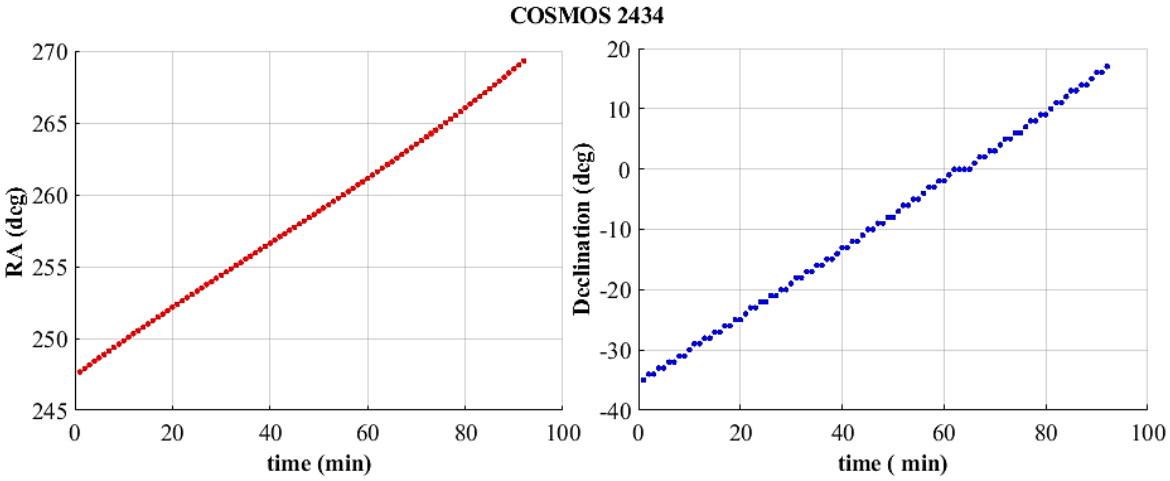

Figure 1– The angular measurements of COSMOS 2434, August 7, 2021.

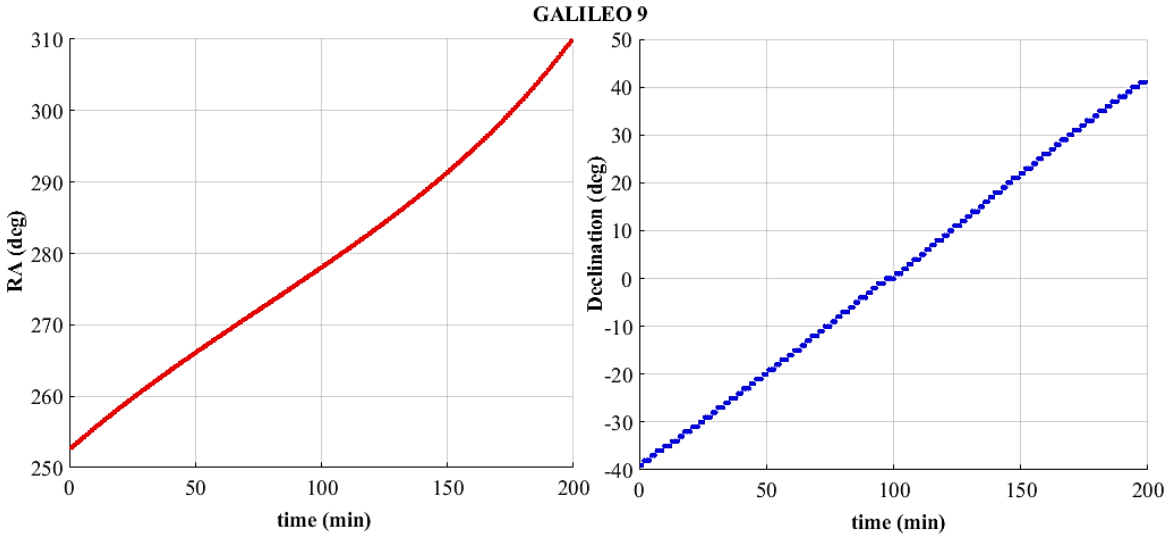

Figure 2 – The angular measurements of GALILEO 9 (205), November 7, 2021.

The acquired images undergo processing techniques to extract accurate position measurements of the space object, the orbit determination process begins with an initial estimate of the satellite's state vector, including parameters like position, velocity, and other orbital elements if applicable [20]. To determine the right ascension and declination of the observed object, The APEX II software package is used [4], and software code simulations in Python.

Figures 1 to 4 provide a comprehensive overview of the angular measurements obtained for each specific celestial object under investigation. These measurements are essential for comprehending the spatial dynamics and observational characteristics of the celestial bodies.

Specifically, Figure 5 visually represents the focal objects of this study, which were carefully observed and recorded from our OSTS Station. The incorporation of Figure 5 is intended to offer a holistic view of the chosen objects, thereby enriching the overall understanding of their trajectories, positions, and behaviors as depicted in our observational data.

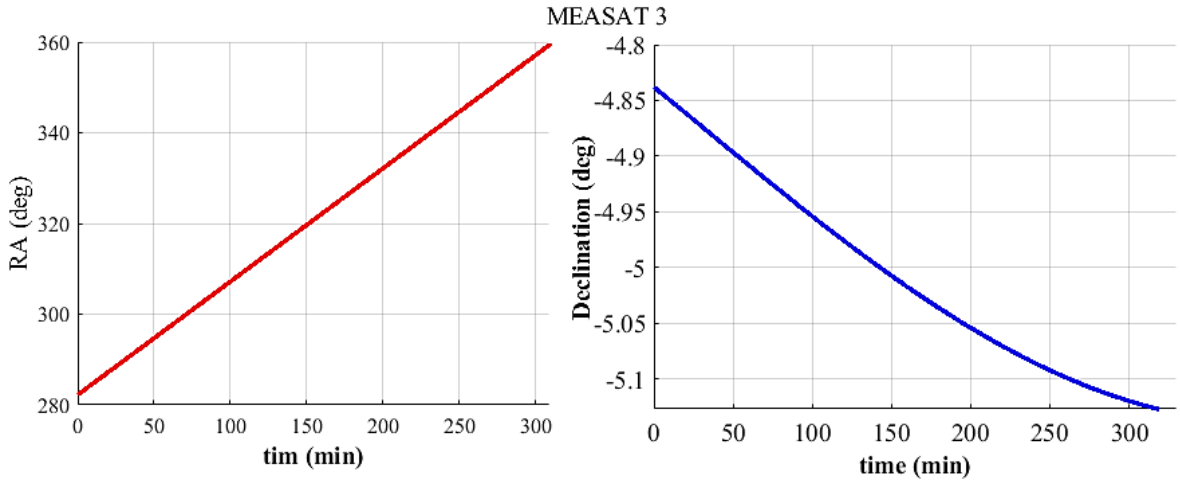

Figure 3 – The angular measurements of MEASAT 3, August 30, 2021.

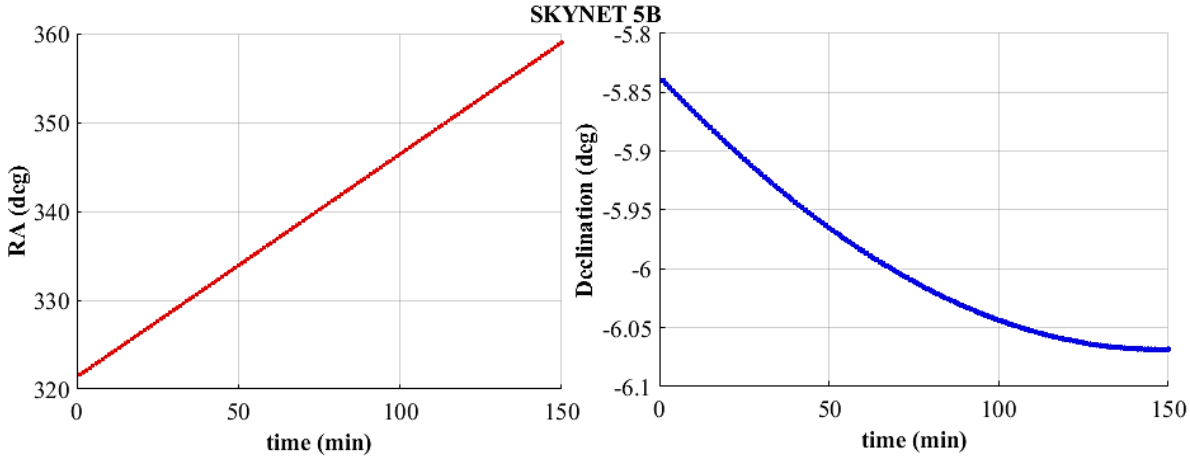

Figure 4 – The angular measurements of SKYNET 5B, November 28, 2021.

The accuracy of filter estimates at different high altitudes was assessed by calculating the average trajectory. The results for Medium Earth Orbit and Geostationary Earth Orbit satellites are presented in Figures 6A-9A and Table 2, illustrating the root mean square position in Earth-cantered inertial coordinates. The Extended Semi-analytical Kalman Filter and the Unscented Semi-analytical Kalman Filter were compared in terms of their performance.

Furthermore, Figures 6B to 9B, along with Table 3, present the Root Mean Square velocity in Earth-cantered inertial (ECI) coordinates for both Medium Earth Orbit and Geostationary Earth Orbit satellites. These visualizations and tabulated results collectively offer a comprehensive overview of the achieved accuracy by both the Extended Semi-analytical Kalman Filter and the Unscented Semi-analytical Kalman Filter. The assessment is conducted across various altitudes, providing a thorough understanding of the filters' performance in different orbital scenarios.

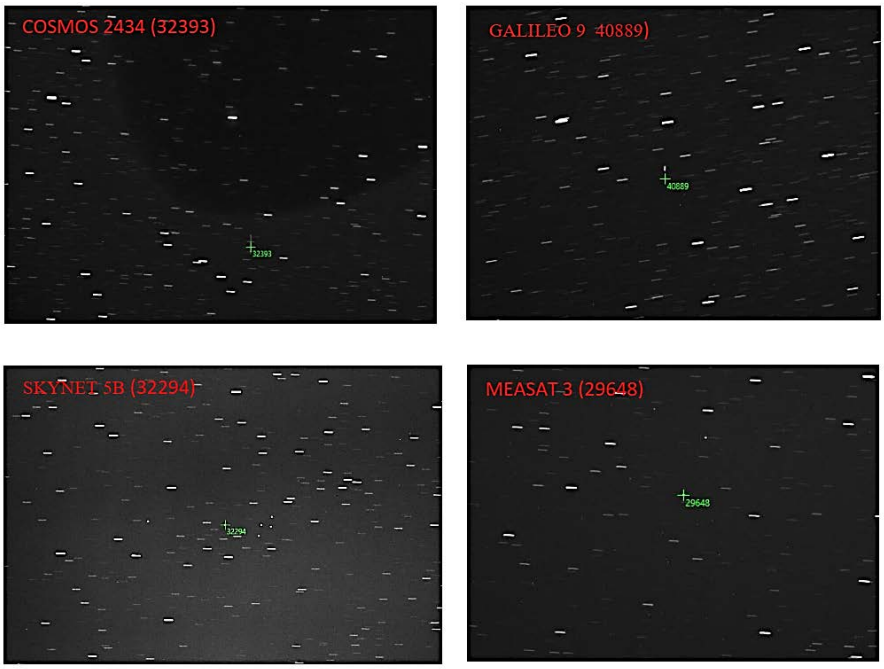

Figure 5 – The objects observed in this study from the OSTS Station Observations taken throughout 7-11/2021.

Table 2 – A comparison of position between ESKF and USKF.

Satellites	Initial	ESKF (RMS) km	USKF (RMS) km
COSMOS 2434 (32393)	25518.11	3.832 (0.01501%)	6.751 (0.0264%)
GALILEO 9 (205) (40889)	29591.43	2.319 (0.0078%)	2.747 (0.0092%)
MEASAT 3 (29648)	42262.73	14.853 (0.0351%)	4.840 (0.011%)
SKYNET 5B (32294)	42172.04	35.477 (0.08412%)	10.024 (0.0237%)

Table 3 – A comparison of velocity between ESKF and USKF.

Satellites	Initial	ESKF (RMS) km/sec	USKF(RMS) km/sec
COSMOS 2434 (32393)	3.951446	0.00223 (0.0564%)	0.00128 (0.0323%)
GALILEO 9 (205) (40889)	3.670704	0.0066461 (0.1810%)	0.0076156 (0.2074%)
MEASAT 3 (29648)	3.379457	0.002924 (0.0865%)	0.002606 (0.0771%)
SKYNET 5B (32294)	3.074172	0.00363 (0.1180%)	0.003593 (0.1168%)

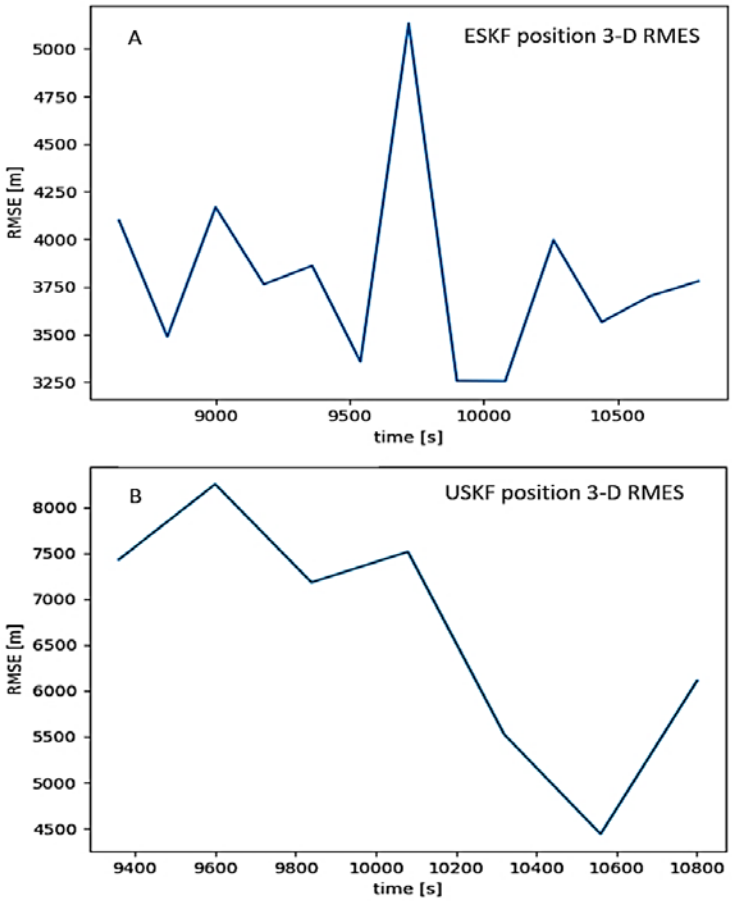

Figure 6A – ECI Root Mean Square Position Analysis for COSMOS 2434 – 08/07/2021

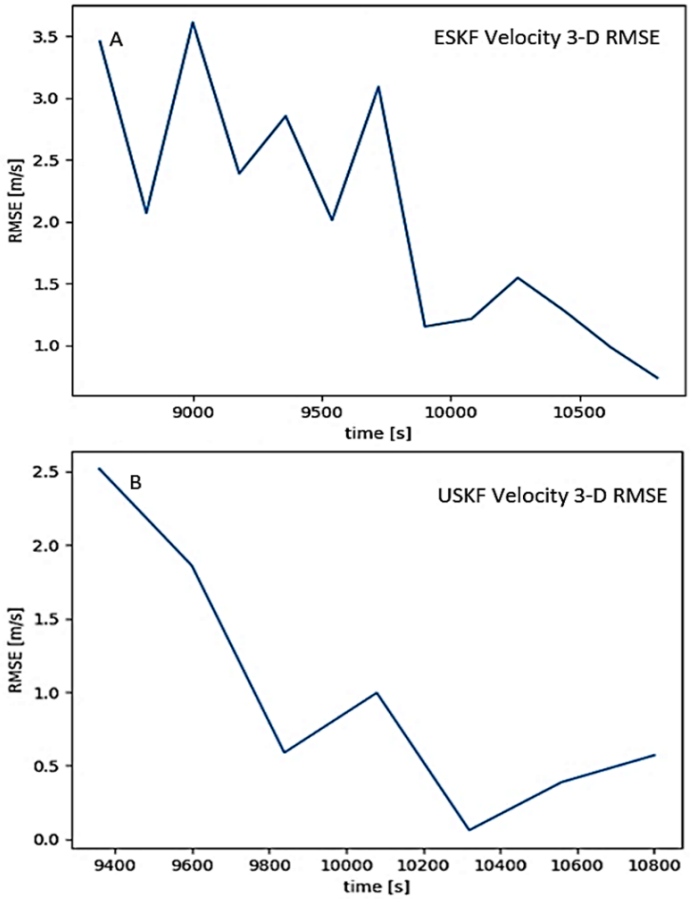

Figure 6B — ECI Root Mean Square Velocity Analysis for COSMOS 2434 – 08/07/2021.

Figures 6A and B comprehensively show the Root Mean Square position and velocity analysis for the COSMOS 2434 satellite in the Earth-centered inertial reference frame. The observations for this analysis were specifically taken on 08/07/2021 at 18:00:00 from the OSTS Observatory. In the upper part of the figure, we observe the results obtained from processing the data using the Extended Kalman Filter. The ESKF is a recursive algorithm that refines estimating the satellite's position over time, incorporating measurements and adjusting predictions. Conversely, the lower part of Figure 6A showcases data processed through the Unscented Kalman Filter. The USKF, another advanced filtering technique, provides an alternative perspective on the satellite's RMS position. It is designed to handle nonlinearities more effectively, making it a valuable tool in situations where traditional linear filters may fall short.

Figures 7A and 7B present a detailed analysis of the Root Mean Square position and velocity of the MEO GALILEO 9 satellite. In Figure 7A, the RMS position is showcased, providing a measure of the average deviation of the satellite's position from its predicted or reference location. This information is crucial for assessing the accuracy and precision of the satellite's orbital path in Medium Earth Orbit. Moving on to Figure 7B, the focus shifts to the satellite's velocity. Understanding the RMS velocity is essential for evaluating how consistently and predictably the satellite is moving through its orbital trajectory.

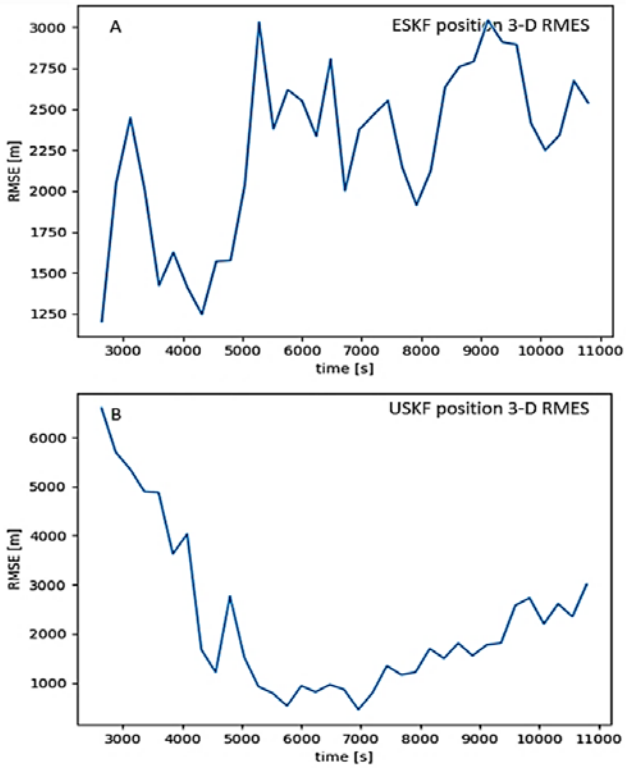

Figure 7A – ECI Root Mean Square position Analysis for GALILEO 9- 11/07/2021

.

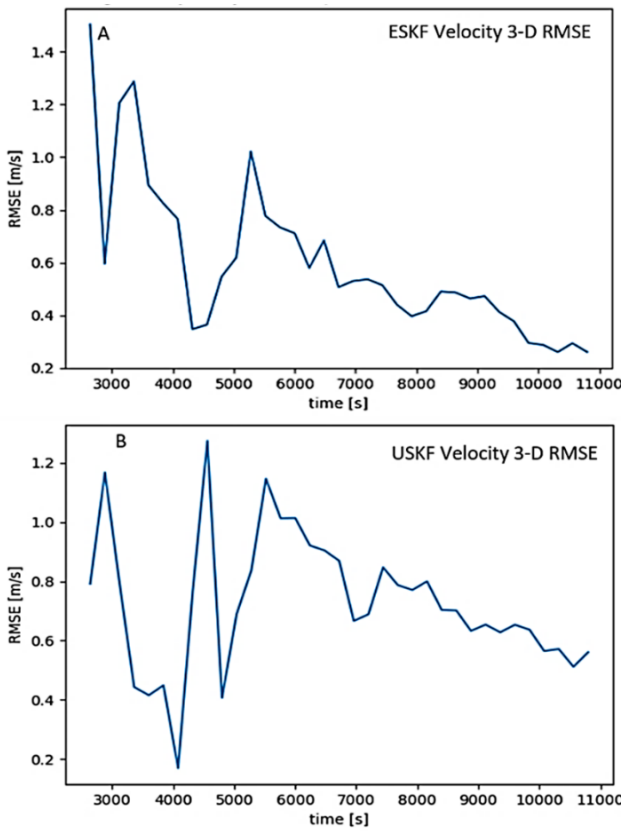

Figure 7B – ECI Root Mean Square Velocity Analysis for GALILEO 9- 11/07/2021.

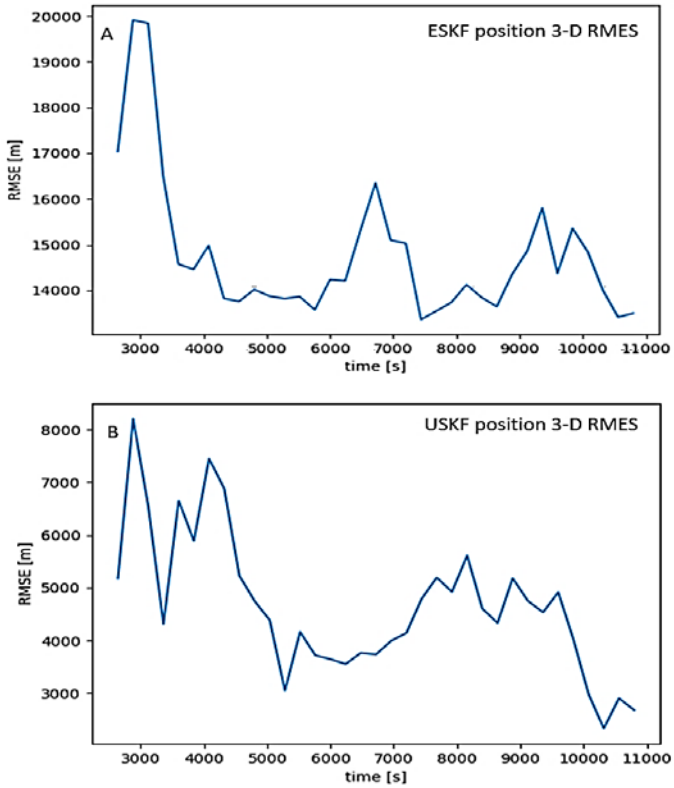

Figure 8A – ECI Root Mean Square position Analysis for MEASAT 3- 30/08/2021

In Figures 8A, 8B, 9A, and 9B, we delve into a comprehensive analysis of the Root Mean Square position and velocity of two crucial satellites: GEO MEASAT 3 and SKYNET 5B. These satellites operate in Geostationary Earth Orbit, and understanding their position and velocity dynamics is fundamental for various applications, including telecommunications and Earth observation. Figure 8A focuses on the RMS position of GEO MEASAT 3, providing insights into the average deviation of its orbital location from the predicted values. Concurrently, Figure 8B extends this analysis to include the RMS velocity, shedding light on the satellite's consistent motion within its orbital path.

In Figures 9A and 9B, the same level of scrutiny is applied to the SKYNET 5B satellite. Figure 9A concentrates on the RMS position, offering a detailed perspective on how closely the satellite adheres to its expected orbital coordinates. Figure 9B complements this by examining the RMS velocity, allowing for a thorough evaluation of the satellite's speed and motion characteristics in the GEO.

To generate measurement data, the Monte Carlo method was employed to ascertain bias values and evaluate estimation errors. Throughout the experimentation, the SGP4 propagation method was consistently applied, with a specific focus on understanding the influence of bias values on orbit determination. The Bias estimation technique played a pivotal role in pinpointing bias values within the measurement data. Subsequent analysis of simulation results from the test case provided insights into the dynamic evolution of absolute errors in 3D position and velocity over a 3-hour simulation period. A careful examination of the results highlighted a comparable performance between the USKF and ESKF propagators.

In particular, both propagators demonstrated position and velocity errors peaking at 4 km and 0.1 m/s, respectively, during a 3-hour Medium Earth Orbit propagation. Additionally, for a 3-hour Geostationary Earth Orbit propagation, errors reached 10 km and 0.3 m/s. The key takeaway from the study was the significant enhancement in the accuracy of orbital estimates across all conducted simulations. Notably, the USKF exhibited a faster convergence to the true trajectory when compared to the ESKF, further validating its efficacy in improving the precision of orbital predictions.

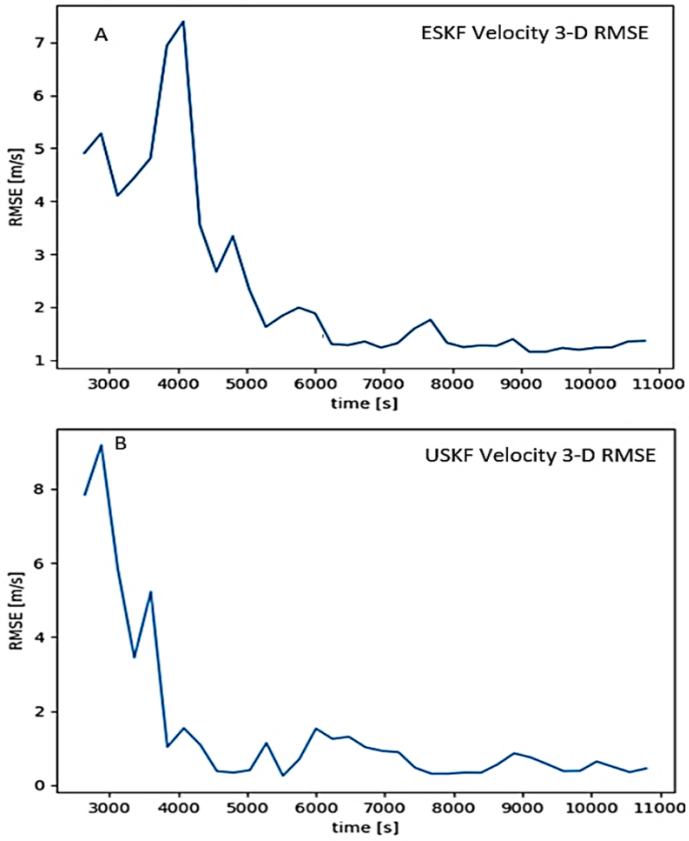

Figure 8B – ECI Root Mean Square Velocity Analysis for MEASAT 3- 30/08/2021.

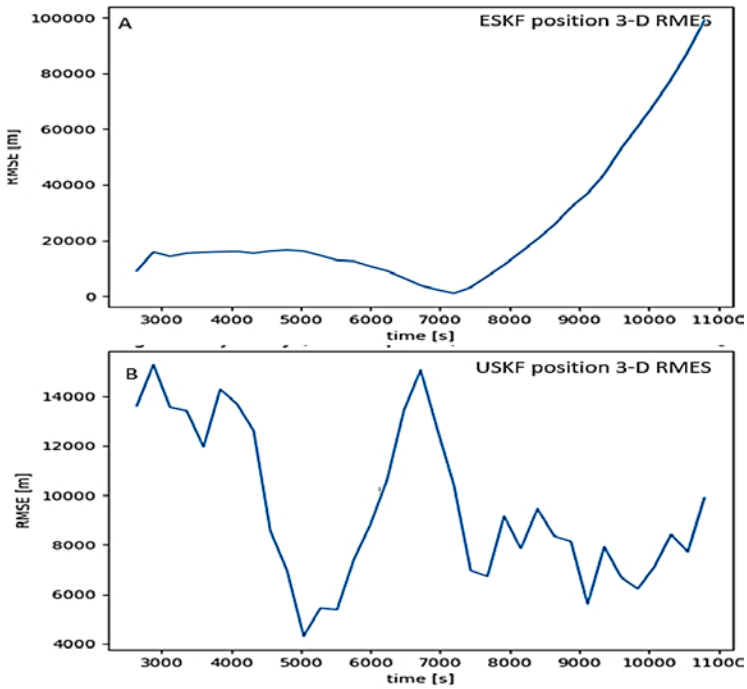

Figure 9A – ECI Root Mean Square position Analysis for SKYNET 5B- 28/11/2021.

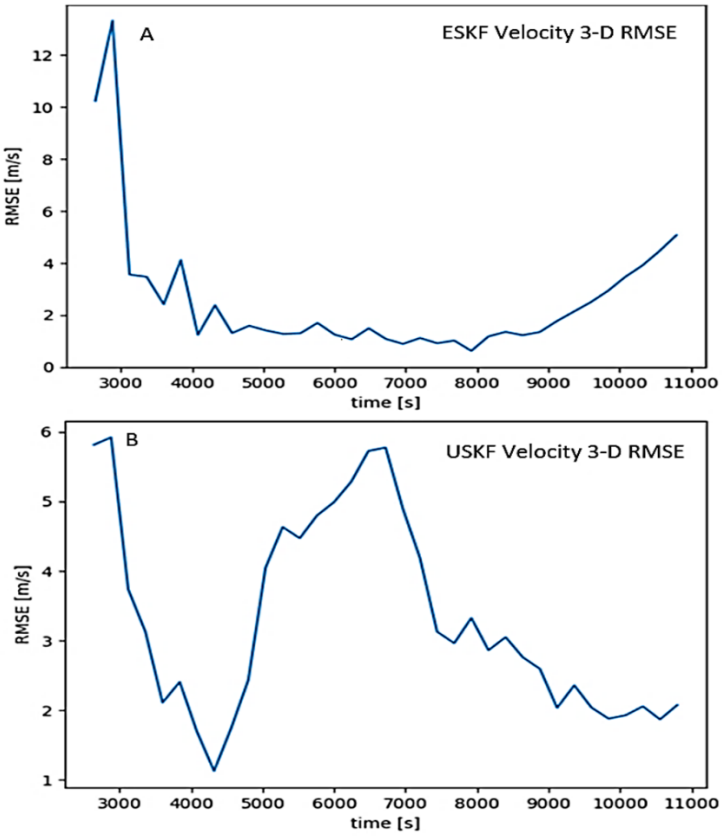

Figure 9B – ECI Root Mean Square Velocity Analysis for SKYNET 5B- 28/11/2021.

The findings underscore the remarkable efficacy of the Unscented Semi-Analytical Kalman Filter when extending a semi-analytical propagation model, particularly in adeptly handling non-linearities inherent in orbit determination. Leveraging the unscented transformation, the USKF achieves a more precise representation of the probability distribution, adeptly capturing the intricate dynamics of dynamic systems. Moreover, the USKF proves highly effective in mitigating the influence of outliers and noise, a critical attribute in satellite tracking scenarios where observational data may encounter disruptions. Notably, the USKF demonstrates a notably swifter convergence rate compared to the Extended Kalman Filter, thereby alleviating computational demands and facilitating efficient real-time orbit determination.

Conclusion

This study explores the orbit estimation of medium earth orbit and geostationary earth orbit satellites based on ground station data. The mean orbital state dynamics were accurately modeled using Semi-analytical orbital propagators, taking into account the practical applications of these satellites. The research demonstrated that the implemented Semi-analytical orbital propagators were not only feasible but also effective when compared to the Extended Kalman Filters, specifically employing unscented Kalman filters. The integration of a smoother was successfully executed and validated for both the ESKF and USKF methods. The simulation outcomes revealed superior performance by the USKF method in comparison to the ESKF method. Notably, the ESKF method exhibited more outliers in certain experiments, underscoring the efficacy of the USKF method in handling and mitigating uncertainties in the estimation process. Overall, this research highlights the practicality and effectiveness of Semi-analytical orbital propagators and demonstrates the advantages of employing the USKF method for improved accuracy in orbit estimation over the ESKF method.

References

1. Abdelaziz A. M., Ibrahim M., Liang Zh., Dong X., and Tealib S. K. "Orbit Predictions for Space Object Tracked by Ground-Based Optical and SLR Stations." *Remote Sensing* 14, no.18 (2022): 4493.

2. Abdelaziz A. M., Tealib S. K., and Molotov I. "Analytical study of Egyptian TIBA-1 satellite orbit from Optical Satellite Tracking Station (OSTS), NRIAG-Egypt." *Astrophysics and Space Science* 366, no.8(2021): 81.

3. Abdel-Aziz Y., Abdelaziz A.M., Tealib S.K., Attia G.F., Molotov I., Schmalz S. "First optical satellite tracking station (OSTS) at NRIAG-Egypt." *New Astronomy* 77 (2020): 101361.

4. Devyatkin, A. V., Gorshanov D. L., Kouprianov V. V., and Verestchagina I. A.. "Apex I and Apex II software packages for the reduction of astronomical CCD observations." *Solar System Research* 44 (2010): 68-80.

5. Escobal P. "Methods of orbit determination." *New York: Wiley.* (1970).

6. Folcik Z. J. "Orbit determination using modern filters/smoothers and continuous thrust modeling." *PhD diss., Massachusetts Institute of Technology*, (2008).

7. Green A. J. "Orbit determination and prediction processes for low altitude satellites." *PhD diss., Massachusetts Institute of Technology*, (1979).

8. Jingshi T., Wang H., Chen Q., Chen Zh., Zheng J., Cheng H., and Liu L. "A time-efficient implementation of Extended Kalman filter for sequential orbit determination and a case study for onboard application." *Advances in Space Research* 62, no. 2 (2018): 343-358.

9. Xingyu Zh., Wang Sh., and Qin T. "Multi-Spacecraft Tracking and Data Association Based on Uncertainty Propagation." *Applied Sciences* 12, no. 15 (2022): 7660.

10. Matteo L., Principe G., Armellin R., Pirovano L., Gondelach D., San J. F., Lara J.M., Gonzalez R. D., Caballero F. P., and Urdampilleta I. "Differential Algebra-based Orbit Determination with the Semi-analytical Propagator SADA." In *8th European Conference on Space Debris*. (2021).

11. Moreira de Oliveira, Rodrigo. Orbit Determination for Low-Altitude Satellites Using Semianalytical Satellite Theory Aerospace Engineering Examination Committee.Master's thesis, *TECNICO LISPOA*. (2021).

12. Henson, Michael A., and Dale E. Seborg. *Nonlinear process control*. Upper Saddle River, New Jersey: Prentice Hall PTR, (1997).

13. Taylor, Stephen Paul. "Semianalytical satellite theory and sequential estimation." *PhD diss., Massachusetts Institute of Technology*, (1982).

14. Teixeira, Bruno OS, Mario A. Santillo, R. Scott Erwin, and Dennis S. Bernstein. "Spacecraft tracking using sampled-data Kalman filters." *IEEE Control Systems Magazine* 28, no. 4 (2008): 78-94.

15. Vallado, David A. *Fundamentals of astrodynamics and applications*. Vol. 12. Springer Science & Business Media, (2001).

16. Schrama, Ernst. "Precision orbit determination performance for CryoSat-2." *Advances in Space Research* 61, no. 1 (2018): 235-247.

17. Van Der Merwe, Rudolph, and Eric A. Wan. "The square-root unscented Kalman filter for state and parameter estimation." *In 2001 IEEE international conference on acoustics, speech, and signal processing. Proceedings (Cat. No. 01CH37221)*, vol. 6, (2001): 3461-3464. I

18. Woodburn, J. and Coppola V. "Analysis of Relative Merits of Unscented and Extended Kalman Filter in Orbit Determination." (1999).

19. Vetter J. R. "Fifty years of orbit determination." *Johns Hopkins APL technical digest* 27, no. 3 (2007): 239.

20. Wagner E. A., "Application of the Extended Semi analytical Kalman Filter to synchronous orbits", *Advances in the Astronautical Sciences*, vol. 54, (1984): 1265–1285.

21. https://www.space-track.org/#gp.